EG UK Computer Graphics & Visual Computing (2018)
G. Tam and F. Vidal (Editors)

Evolutionary interactive analysis of MRI Gastric images using a multiobjective cooperative-coevolution scheme

S. F. Al-Maliki[1,2], É. Lutton[3], F. Boué[3,4] and F. P. Vidal[1]

[1]Bangor University, United Kingdom
[2]Basrh University, Iraq
[3] INRA-AgroParisTech, France
[4] LLB, CEA CNRS, France

Abstract

In this study, we combine computer vision and visualisation/data exploration to analyse magnetic resonance imaging (MRI) data and detect garden peas inside the stomach. It is a preliminary objective of a larger project that aims to understand the kinetics of gastric emptying. We propose to perform the image analysis task as a multi-objective optimisation. A set of 7 equally important objectives are proposed to characterise peas. We rely on a cooperation co-evolution algorithm called 'Fly Algorithm' implemented using NSGA-II. The Fly Algorithm is a specific case of the 'Parisian Approach' where the solution of an optimisation problem is represented as a set of individuals (e.g. the whole population) instead of a single individual (the best one) as in typical evolutionary algorithms (EAs). NSGA-II is a popular EA used to solve multi-objective optimisation problems. The output of the optimisation is a succession of datasets that progressively approximate the Pareto front, which needs to be understood and explored by the end-user. Using interactive Information Visualisation (InfoVis) and clustering techniques, peas are then semi-automatically segmented.

CCS Concepts

•Human-centered computing → Visualization application domains; •Computing methodologies → Search methodologies; Graphics systems and interfaces; •Applied computing → Life and medical sciences;

1. Introduction

Digestion is known to be much more complex than simple food decomposition and absorption of macro-nutrients, e.g. carbohydrates, proteins and lipids, as well as micro-nutrients, e.g. vitamins, minerals, and other food components. Two aspects have been recognised as relevant: kinetics of digestion and food structure [BMLG*13, BBH*13, MGG*13, DCGRP*14, ZHH13].

The work presented here is a contribution to a large project focused on the understanding of the influence of food structure on digestion. Our approach is based on advanced imaging techniques to observe phenomena at different scales. We rely on magnetic resonance imaging (MRI) of the gastrointestinal tract (GIT) for capturing *in vitro* large scale information, while smaller scale measurements are performed *in vitro* on large facilities (small-angle neutron scattering (SANS), small-angle X-ray scattering (SAXS), and X-ray imaging) [FBT*18, LTLF*17]. The observation of *in vivo* digestion using MRI is a recent challenge. Here the focus is on the content of the GIT and not on the GIT itself as in clinical routine [MG13, RAD*06, SSF06].

Thanks to this multi-disciplinary collaboration, we recently acquired experimental MRI data of the stomach and duodenum area of healthy human volunteers. The aim is to analyse the content of the stomach and its evolution. We focus here on the kinetics of gastric emptying for two species of ingested food: i) progressively and partially digested cooked pasta, and ii) frozen garden peas, which keep their shape in early gastric stages (see Fig. 1).

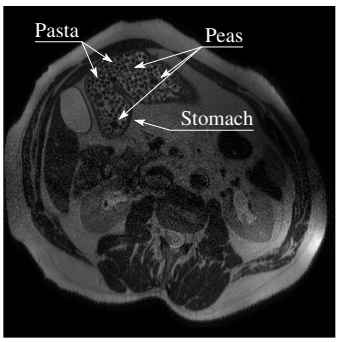

Figure 1: *MRI slice of a human stomach containing peas and pasta.*

DOI: 10.2312/cgvc.20181216

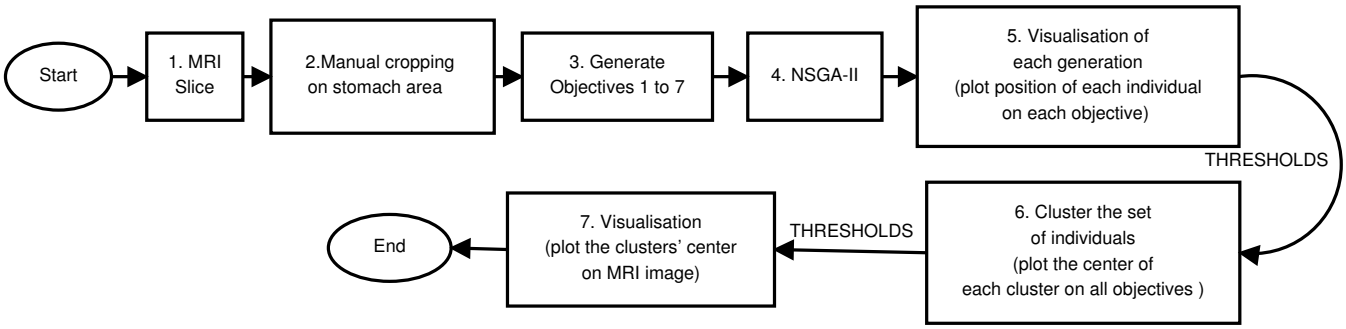

Figure 2: *Overall flowchart of our image analysis and information visualisation pipeline.*

Manually processing this large amount of MRI data sets is not practically feasible. Processing it in a fully-automatic manner is not trivial as appropriate information need first to be collected and analysed to provide suitable models. Here we show how a "Fly Algorithm" [VLLR09] can be efficiently adapted to analyse these MRI images. The Fly Algorithm, on the contrary to classical image processing techniques, is able to provide a map of various features (e.g. the location of components of the food bolus). In this paper, we present early results on the tracking of peas (around 20 peas in one stomach for the current experimental data), which reveals the motion of the stomach (the food bolus is stirred and gently "triturated" for better action of the gastric juice). For this purpose, the Fly Algorithm has been turned into a multi-objective cooperative-coevolution algorithm, and expert knowledge has been integrated through an interaction/visualisation interface. The combination of visualisation and evolutionary computing is still a relatively overlooked field. Two main approaches are currently explored:

- visualisation to understand evolutionary algorithms (EAs) behaviour [WJB*99, Poh99, WSL04, KE05], or outputs [BTT*17];
- interactive artificial evolution to improve the visualisation [BSLF13, LPT16, HM17].

We show how simple, but yet effective, Information Visualisation (InfoVis) techniques can be used to display the output of an evolutionary algorithm. In particular, the multi-objective scheme provides complex time series of Pareto front data, which needs to be understood and explored by the end-user. Fig. 2 summarises our processing pipeline.

2. Problem definition

In Step 1 of Fig. 2, we selected a typical MRI image containing the stomach full of pasta and peas. The MRI slice is manually cropped to only focus on the stomach and its content (see Step 2). In Step 3, we aim to describe what a pea looks like and how to mathematically model it:

- Peas keep their shape and size in early gastric stages. A pea appear as a circle of a fixed radius of about 4mm, which is equivalent to $R = 8$ pixels.
- The interior of a pea is homogeneous; the outside is not.

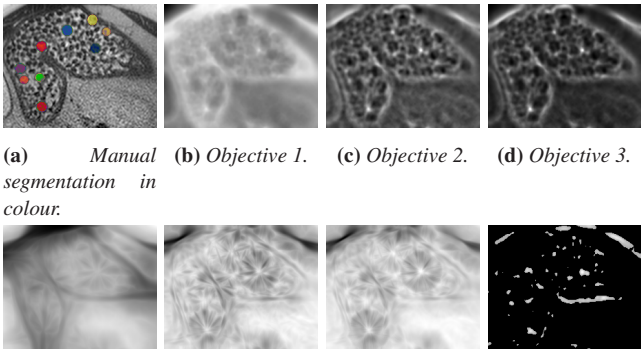

(a) *Manual segmentation in colour.* **(b)** *Objective 1.* **(c)** *Objective 2.* **(d)** *Objective 3.*

(e) *Objective 4.* **(f)** *Objective 5.* **(g)** *Objective 6.* **(h)** *Objective 7.*

Figure 3: *Objectives. For visibility objective functions are displayed in negative (low intensities appear bright; high intensities appear dark).*

- The interior of a pea is darker than the outside.

We propose to implement this knowledge into 7 equally important objectives to minimise as a multi-objective optimisation problem (see Step 2. in figure 2).

For each pixel (x,y) of the MRI image, Objective 1 measures the local pixel intensity standard deviation (σ) within a circular region of interest (ROI):

$$obj1(x,y,I,R) = \sigma(ROI_C(I,x,y,R)) \quad (1)$$

where $ROI_C(I,x,y,R)$ is a circular region of interest in Image I. It is centred on Pixel (x,y), and its radius is R. Fig. 3b is an image representation of Objective 1.

Objective 2 measures how homogeneous the interior of the circle is and how heterogeneous the outside is (see Fig. 3c). It compares Objective 1 with the local pixel intensity standard deviation within a ring region of interest (ROI_R) whose inner radius is R and outer radius $R+5$:

$$obj2(x,y,I,R) = obj1(x,y,I,R) - \sigma(ROI_R(x,y,I,R,R+5)) \quad (2)$$

Objective 3 combines Objectives 1 and 2 (see Fig. 3d):

$$obj3(x,y,I,R) = obj1(x,y,I,R) \times obj2(x,y,I,R) \quad (3)$$

When a pea is considered in Objectives 1, 2 and 3, the corresponding pattern in Figures 3b, 3c and 3d is isotropic. Each pea corresponds to a small bright dot onto a dark background in these images. Objectives 4, 5 and 6 exploit this property. We model an intensity profile ($defP$) of 30 pixels using a triangular function. It mimics an intensity profile perfectly centred on a pea:

$$defP(i) = \begin{cases} 1 - \frac{|i-(2R-1)|}{R-1}, & \forall i \in \left[\frac{30}{2} - R, \frac{30}{2} + R\right] \\ 0, & \text{otherwise} \end{cases} \quad (4)$$

For each pixel in Figures 3b, 3c and 3d, we extract 89 intensity profiles ($prof_k$) every 2° around that pixel:

$$obj_{iso}(x,y,I) = -\max\left(\sum_{i=0}^{i<30} (defP(i) - prof_k(I,x,y,i))^2\right) \quad \forall k \in [0,89) \quad (5)$$

where $prof_k(I,x,y,i)$ is i-th value of the intensity profile in Image I, centred of Pixel x,y at the k-th angle.

$$obj4(x,y) = obj_{iso}(x,y,obj1) \quad (6)$$
$$obj5(x,y) = obj_{iso}(x,y,obj2) \quad (7)$$
$$obj6(x,y) = obj_{iso}(x,y,obj3) \quad (8)$$

Objective 7 assesses that the interior of the circle is darker than the ring around it:

$$f(x,y) = \overline{ROI_C}(x,y,I,R-1) - \overline{ROI_R}(x,y,I,R-1,R+5)$$
$$obj7(x,y) = \begin{cases} f(x,y), & \forall f(x,y) \leq T \\ 0, & \text{otherwise} \end{cases} \quad (9)$$

where $\overline{ROI_C}$ is the average pixel value of a given circular ROI, $\overline{ROI_R}$ is the average pixel value of a given ring ROI, and T is a user defined threshold. $obj7(x,y)$ is expected to be negative or null, which is suitable for a minimisation algorithm. T is also negative. It restricts non-null values in $obj7$ to areas where the difference in pixel intensities of the two corresponding ROIs are significantly different, which correspond to the location of peas and stomach wall.

3. Multi-objective optimisation problem

Pea detection is actually a non-trivial optimisation problem, as it involves multiple objectives that cannot be merged into a single one using simple rules (example: a circular uniform area & a defined colour & and an irregular background ...) and/or subjective preference weights. Multi-objective optimisation considers all objectives as equally important and non comparable. It provides a set of trade-off between objectives, the Pareto front. The Pareto front is the set of non-dominated solutions, i.e. points of the search space for which one objective function cannot be improved in value without degrading some of the other objectives [Mie98].

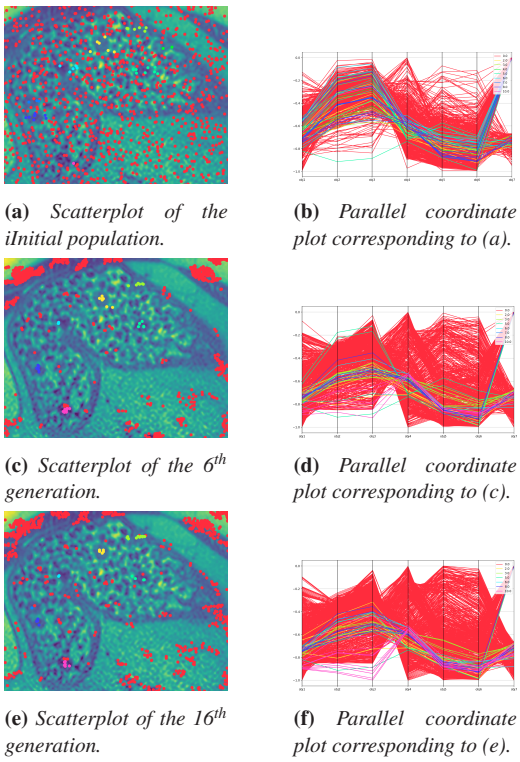

(a) *Scatterplot of the iInitial population.*

(b) *Parallel coordinate plot corresponding to (a).*

(c) *Scatterplot of the 6th generation.*

(d) *Parallel coordinate plot corresponding to (c).*

(e) *Scatterplot of the 16th generation.*

(f) *Parallel coordinate plot corresponding to (e).*

Figure 4: *Scatterplots and parallel coordinates plots of successive generations. All solutions (flies) are plotted in red by default. When the user selects an area in the scatterplot, a specific colour is assigned to this area and linked to the corresponding lines in the parallel coordinate plot.*

Evolutionary optimisation methods can be adapted to deal with multiple objectives, and various efficient algorithms are now available. NSGA-II [DPAM02] is a very popular implementation, that is able to produce an efficient sampling of the Pareto front in a single run of the algorithm.

Here, we implement a multi-objective version of the Fly Algorithm based on NSGA-II so that the population of flies stabilises onto a Pareto front (see Step 4 in Fig. 2). 1000 individuals are used over 25 generations. For up-to-date details on the Fly Algorithm, see `https://en.wikipedia.org/wiki/Fly_algorithm`. Once a Pareto front (i.e. a set of possible best solutions) is produced, the decision may be put in the hand of an expert.

4. Visualisation

The output of Step 4 of the flowchart (Fig. 2) is a dataset of 1000×25 samples, i.e. (x,y) positions with 7 associated fitness values. In typical multi-objective evolutionary algorithms (EAs), one of the individual on the Pareto front is a possible answer to the optimisation problem. The Fly Algorithm approach provides a set of points as a solution, each point corresponding not only to a possible pea location, but also to a different objective priority assessment. Several flies of the population may co-exist on the

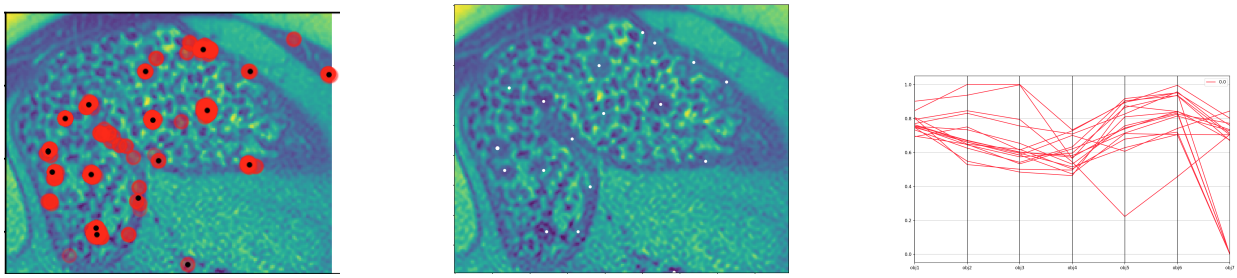

(a) *Clusters.* **(b)** *Cluster centres.* **(c)** *Parallel coordinate plot.*

Figure 5: *Candidate solution clusters.*

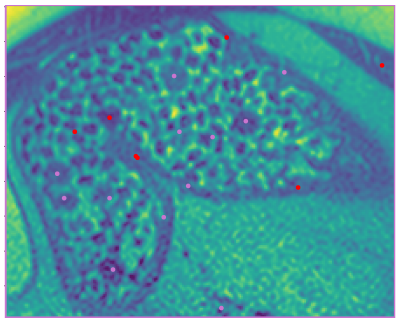

Figure 6: *Final result.*

same pea with different objective weights. Automatically extracting the points that really correspond to peas is not trivial. Extracting only one point per pea, the point the closest to the centre of the corresponding pea, is even more complicated. This can be done efficiently through an interactive visualisation interface.

In Step 5 of Fig. 2, each generation is subsequently displayed twice at a time. A scatterplot is used to display the position of the individuals over the MRI image (see left-hand side column of Fig. 4). A parallel coordinate plot is used to display the values of the multiple objective functions corresponding to each individual (see right-hand side column of Fig. 4). This plot represents a point in a n-dimensional space as a broken line with $n-1$ segments, joining its n coordinates located on n vertical axes. The user can easily and interactively select areas of points in the scatterplot that correspond to peas. Each new manually selected area is assigned a new unique colour, which is the same in both plots. With this tool, the behaviour of individuals toward a global optimal solution in each generation can be visually detected. It also helped us understand the relationship between positions in peas and objective functions. The result is used to define 7 validity ranges (two thresholds per objective) that filter out the 25,000 individuals generated during the evolutionary process. Only the individuals meeting all 7 validity ranges are considered in the following steps, others are discarded.

In Step 6 of Fig. 2, groups of points in the 2-D space are identified using clustering based on a Gaussian Mixture Model (GMM) (see Fig. 5a). Clusters that are close to each other (e.g. within a pea diameter) are then merged into a single cluster. All the cluster centres are extracted and presented to the user (see Fig. 5b). Using another parallel coordinate plot a new set of thresholds is extracted (see Fig. 5c). It is used in the following step to further refine the results and limit the number of false positive (i.e. points that do not actually correspond to peas).

Step 7 of Fig. 2 outputs the final result. In total, 19 points were selected. The last set of thresholds is used so that stronger candidates are highlighted using a purple dot in Fig. 6; weaker candidates using a red dot. 9 peas were manually selected in Fig 3a. Note that the selection is depended on a personal vision. It is unclear if some points near the wall of the stomach correspond to peas or not. 7 peas were highlighted in purple; 2 in red.

5. Conclusions

In this short paper, we presented some preliminary results of our semi-automatic evolutionary segmentation of garden peas in MRI images. To our knowledge, we proposed the first multi-objective implementation of the Fly Algorithm. An interactive visualisation, combining image display, scatter plot and parallel coordinate plot, is used to analyse the output of the evolutionary algorithm. It helps us understanding the complex relationship between the objectives and extracting individuals of the Pareto front that correspond to peas. This research can be extended to segment other structures which cannot be identify by a single equation.

In future work, a more robust and comprehensive evaluation will be performed. this tool will be integrated into a machine learning (ML) framework to assist domain experts in the provision of training data for a deep neural network. This way, it is possible to address some issues related to sparse data that can prevent the use of ML methods. The latter require a lot of manually labelled medical images. This is a time consuming task for domain experts, but mandatory to provide enough data for learning process. A comparison with other algorithms and a robust validation study will be provided in future developments of the method.

Acknowledgements

The authors are grateful to Xavier Maître and Luc Darrasse of the IR4M CNRS/Orsay University at CEA-SHFJ who performed the MRI measurements. This work has been done in the framework of the PhD (IDI/Paris Saclay) of Daniela Freitas.

Acronyms

EA evolutionary algorithm.
EAs evolutionary algorithms.
GIT gastrointestinal tract.
GMM Gaussian Mixture Model.
InfoVis Information Visualisation.
ML machine learning.
MRI magnetic resonance imaging.
ROI region of interest.
SANS small-angle neutron scattering.
SAXS small-angle X-ray scattering.

References

[BBH*13] BAX M.-L., BUFFIÈRE C., HAFNAOUI N., GAUDICHON C., SAVARY-AUZELOUX I., DARDEVET D., SANTÉ-LHOUTELLIER V., RÉMOND D.: Effects of meat cooking, and of ingested amount, on protein digestion speed and entry of residual proteins into the colon: A study in minipigs. *PLOS ONE 8*, 4 (Apr. 2013), 1–7. doi:10.1371/journal.pone.0061252. 1

[BMLG*13] BARBÉ F., MÉNARD O., LE GOUAR Y., BUFFIÈRE C., FAMELART M.-H., LAROCHE B., LE FEUNTEUN S., DUPONT D., RÉMOND D.: The heat treatment and the gelation are strong determinants of the kinetics of milk proteins digestion and of the peripheral availability of amino acids. *Food chemistry 136*, 3-4 (Feb. 2013), 1203–1212. doi:10.1016/j.foodchem.2012.09.022. 1

[BSLF13] BACH B., SPRITZER A., LUTTON E., FEKETE J.-D.: Interactive Random Graph Generation with Evolutionary Algorithms. In *International Symposium on Graph Drawing (GD 2012)* (Berlin, Heidelberg, 2013), Didimo W., Patrignani M., (Eds.), vol. 7704 of *Lecture Notes in Computer Science*, Springer Berlin Heidelberg, pp. 541–552. doi:10.1007/978-3-642-36763-2_48. 2

[BTT*17] BOUKHELIFA N., TONDA A., TRELEA I.-C., PERROT N., LUTTON E.: Interactive knowledge integration in modelling for food sustainability : challenges and prospects. In *ACM CHI Workshop on Designing Sustainable Food Systems* (NA, France, 2017), p. np. URL: https://hal.archives-ouvertes.fr/hal-01604947. 2

[DCGRP*14] DONATO-CAPEL L., GARCIA-RODENAS C., POUTEAU E., LEHMANN U., SRICHUWONG S., ERKNER A., KOLODZIEJCZYK E., HUGHES E., WOOSTER T., SAGALOWICZ L.: Chapter 14 - technological means to modulate food digestion and physiological response. In *Food Structures, Digestion and Health*, Boland M., Golding M., Singh H., (Eds.). Academic Press, San Diego, 2014, pp. 389–422. doi:10.1016/B978-0-12-404610-8.00014-1. 1

[DPAM02] DEB K., PRATAP A., AGARWAL S., MEYARIVAN T.: A fast and elitist multi-objective genetic algorithm: NSGAII. *IEEE Transactions on Evolutionary Computation 6*, 2 (Aug. 2002), 182–197. doi:10.1109/4235.996017. 3

[FBT*18] FLOURY J., BIANCHI T., THÉVENOT J., DUPONT D., JAMME F., LUTTON E., PANOUILLÉ M., BOUÉ F., FEUNTEUN S. L.: Exploring the breakdown of dairy protein gels during in vitro gastric digestion using time-lapse synchrotron deep-uv fluorescence microscopy. *Food Chemistry 239* (2018), 898–910. doi:10.1016/j.foodchem.2017.07.023. 1

[HM17] HALIM Z., MUHAMMAD T.: Quantifying and optimizing visualization: An evolutionary computing-based approach. *Information Sciences 385-386*, Supplement C (2017), 284–313. doi:10.1016/j.ins.2016.12.035. 2

[KE05] KERREN A., EGGER T.: EAVis: a visualization tool for evolutionary algorithms. In *2005 IEEE Symposium on Visual Languages and Human-Centric Computing (VL/HCC'05)* (Sept. 2005), pp. 299–301. doi:10.1109/VLHCC.2005.33. 2

[LPT16] LUTTON E., PERROT N., TONDA A.: Model analysis and visualization. In *Evolutionary Algorithms for Food Science and Technology* (2016), John Wiley & Sons, Inc., pp. 33–55. doi:10.1002/9781119136828.ch3. 2

[LTLF*17] LUTTON E., THEVENOT J., LE FEUNTEUN S., FLOURY J., PANOUILLE M., DUPONT D., ROBLIN P., BOUE F.: Evolution of food gel structures during simulated gastro-intestinal digestion using small angle scattering at SOLEIL synchrotron. In *5th International Conference on Food Digestion* (2017). URL: https://prodinra.inra.fr/record/394314. 1

[MG13] MASSELLI G., GUALDI G.: CT and MR enterography in evaluating small bowel diseases: when to use which modality? *Abdominal Imaging 38*, 2 (Apr. 2013), 249–259. doi:10.1007/s00261-012-9961-8. 1

[MGG*13] MICHALSKI M.-C., GENOT C., GAYET C., LOPEZ C., FINE F., JOFFRE F., VENDEUVRE J., BOUVIER J., CHARDIGNY J.-M., RAYNAL-LJUTOVAC K.: Multiscale structures of lipids in foods as parameters affecting fatty acid bioavailability and lipid metabolism. *Progress in Lipid Research 52*, 4 (Oct. 2013), 354–373. doi:10.1016/j.plipres.2013.04.004. 1

[Mie98] MIETTINEN K.: *Nonlinear Multiobjective Optimization*, vol. 12 of *International Series in Operations Research & Management Science*. Springer US, 1998. doi:10.1007/978-1-4615-5563-6. 3

[Poh99] POHLHEIM H.: Visualization of evolutionary algorithms - set of standard techniques and multidimensional visualization. In *Proceedings of the 1st Annual Conference on Genetic and Evolutionary Computation - Volume 1* (San Francisco, CA, USA, 1999), GECCO'99, Morgan Kaufmann Publishers Inc., pp. 533–540. 2

[RAD*06] RETO T., ANDREAS S., DOMINIK W., OLIVER G., PETER B., MICHAEL F., WERNER S.: Gastric motor function and emptying in the right decubitus and seated body position as assessed by magnetic resonance imaging. *Journal of Magnetic Resonance Imaging 23*, 3 (Feb. 2006), 331–338. doi:10.1002/jmri.20507. 1

[SSF06] SCHWIZER W., STEINGOETTER A., FOX M.: Magnetic resonance imaging for the assessment of gastrointestinal function. *Scandinavian Journal of Gastroenterology 41*, 11 (2006), 1245–1260. doi:10.1080/00365520600827188. 1

[VLLR09] VIDAL F. P., LOUCHET J., LUTTON E., ROCCHISANI J.: PET reconstruction using a cooperative coevolution strategy in LOR space. In *IEEE Nuclear Science Symposium Conference Record* (Oct. 2009), IEEE, pp. 3363–3366. doi:10.1109/NSSMIC.2009.5401758. 2

[WJB*99] WU A. S., JONG K. A. D., BURKE D. S., GREFENSTETTE J. J., RAMSEY C. L.: Visual analysis of evolutionary algorithms. In *Proceedings of the 1999 Congress on Evolutionary Computation-CEC99 (Cat. No. 99TH8406)* (1999), vol. 2, p. 1425 Vol. 2. doi:10.1109/CEC.1999.782649. 2

[WSL04] WU H.-C., SUN C.-T., LEE S.-S.: Visualization of evolutionary computation processes: from the perspective of population. In *Fifth World Congress on Intelligent Control and Automation (IEEE Cat. No.04EX788)* (June 2004), vol. 3, pp. 2077–2081. doi:10.1109/WCICA.2004.1341950. 2

[ZHH13] ZHU Y., HSU W. H., HOLLIS J. H.: The impact of food viscosity on eating rate, subjective appetite, glycemic response and gastric emptying rate. *PLOS ONE 8*, 6 (June 2013), 1–6. doi:10.1371/journal.pone.0067482. 1